Journal of Biomechanics 177 (2024) 112385

Contents lists available at ScienceDirect

Journal of Biomechanics

journal homepage: www.elsevier.com/locate/jbiomech

Should individuals with unilateral transtibial amputation carry a load on their intact or prosthetic side?

Satria Ardianuari [a,b], Krista M. Cyr [a], Richard R. Neptune [c], Glenn K. Klute [a,b,*]

[a] Department of Veterans Affairs Center for Limb Loss and MoBility, 1660 S. Columbian Way, Seattle, WA 98108, USA
[b] Department of Mechanical Engineering, University of Washington, 3900 East Stevens Way NE, Seattle, WA 98195, USA
[c] Walker Department of Mechanical Engineering, The University of Texas at Austin, 204 East Dean Keeton Street, Austin, TX 78712, USA

ARTICLE INFO

Keywords:
Lower limb amputation
Load carriage
Side load carriage
Gait
Biomechanics
Kinetics

ABSTRACT

Carrying side loads often occurs during activities of daily living. As walking is most unstable mediolaterally, side load carriage may further compromise gait biomechanics, especially for transtibial amputees (TTAs). This study investigated the effects of side load carriage on gait kinetics during steady-state walking to determine which side, intact or prosthetic, TTAs should carry a load. Twelve unilateral TTAs wore a passive-elastic foot and carried a side load of 13.6 kg while walking at their self-selected speed. Kinetic metrics, including ground reaction force peaks and impulses, loading and unloading rates, and joint moments and powers, were analyzed. TTAs had smaller propulsive forces on their intact limb during the prosthetic side load condition. During the intact side load condition, they had smaller hip flexor moment in late stance and smaller knee flexor moment at the end of swing on their intact limb. They had higher hip and knee abductor moments on their intact limb and prosthetic limb in early and late stance during the contralateral side load condition. TTAs generated higher hip extensor power at weight acceptance during the ipsilateral side load. Significant interactions were observed in hip extensor power and abductor moment, suggesting strong associations between hip extensor power generation and the ipsilateral side load and between hip abductor moment and the contralateral side load. These mixed results demonstrate some kinetic changes due to side load carriage and suggest that the side TTAs should carry a load depends on the desired effects, primarily on their intact limb.

1. Introduction

Carrying loads is essential for activities of daily life, from mundane tasks to specialized occupations and recreational pursuits. There are several different ways to carry loads, and each method may have a different effect on an individual's gait biomechanics. Front and back load carriage methods have been shown to induce higher metabolic costs and increase lower limb muscle activity in early stance for healthy individuals (Silder et al., 2013). Front load carriage has also been shown to elevate the risk of falling (Yang et al., 2022). Others have shown that back load carriage can increase hip and knee flexion (Attwells et al., 2006; Harman et al., 1992), alter hip adduction/abduction, hip rotation, and pelvic tilt (Birrell and Haslam, 2009), and reduce stride length and increase cadence (Birrell and Haslam, 2009). Loads may also be carried laterally for convenience over short distances or for intermittent periods, such as carrying a bag over one shoulder or holding a baby or child on one hip while walking. Despite the frequency of side load carriage, there have been little to no biomechanical analyses of gait with this load carriage method, particularly for individuals who exhibit higher fall risk, such as those with a lower-limb amputation.

Individuals without a lower-limb amputation can modulate power generated by the biological ankle to accommodate added loads during walking. Ankle dorsiflexors provide body support in early stance (Anderson and Pandy, 2003). In addition to support, ankle plantarflexors provide essential functions for forward propulsion (Liu et al., 2006; Neptune et al., 2004, 2001), initiation of swing (Neptune et al., 2001), as well as dynamic balance control (Neptune and McGowan, 2016, 2011). Absence of ankle plantarflexors in the residual limb of transtibial amputees (TTAs) may aggravate asymmetrical gait biomechanics and require additional compensatory mechanisms in response to carrying a side load.

TTAs have been shown to experience altered biomechanics, even

* Corresponding author at: Department of Veterans Affairs, Rehabilitation Research and Development, Center for Limb Loss and MoBility, 1660 S. Columbian Way MS-151, Seattle, WA 98108, USA.
E-mail addresses: satria@uw.edu (S. Ardianuari), krista.cyr@va.gov (K.M. Cyr), rneptune@mail.utexas.edu (R.R. Neptune), gklute@uw.edu (G.K. Klute).

https://doi.org/10.1016/j.jbiomech.2024.112385
Accepted 23 October 2024
Available online 28 October 2024
0021-9290/Published by Elsevier Ltd.

during unloaded walking. These changes include higher peak ground reaction force (GRF) in their intact limb (Nolan et al., 2003), which can lead to knee osteoarthritis (Gailey et al., 2008; Norvell et al., 2005; Struyf et al., 2009), chronic low back pain (Highsmith et al., 2019), and chronic lower limb pain (Burke et al., 1978). Further, TTAs have been observed to have increased prosthetic limb hip extensor moment, power, and positive work in early stance (Bateni and Olney, 2002; Gitter et al., 1991; Grumillier et al., 2008; Silverman et al., 2008), and a greater prosthetic limb hip flexor moment in pre-swing (Sadeghi et al., 2001). With added loads, these effects may be magnified. TTAs with passive-elastic feet respond to back load conditions with smaller ankle dorsiflexor moment in the intact limb, smaller hip extensor power in early stance in both limbs, and smaller ankle plantarflexor and knee flexor moment in the prosthetic limb (Doyle et al., 2014). Further, carrying a back load has been shown to affect gait kinematics in TTAs, such as smaller trunk and pelvic range of motion (Doyle et al., 2015, 2014; Schnall et al., 2014) and higher metabolic demand compared to individuals without an amputation (Schnall et al., 2012). Using modeling and simulation, an individual TTA demonstrated a higher dependence on their intact limb to compensate for the higher demands of added front and back loads (Templin et al., 2021).

Effects of load carriage have primarily been studied for front and back load conditions, and thus an understanding of gait biomechanics in TTAs when carrying a side load is still poorly understood. Further, it has been demonstrated that walking is most unstable in the mediolateral direction (Dean et al., 2007; McAndrew et al., 2011). Thus, it remains an open question whether side load carriage would exacerbate the already altered gait kinetics in TTAs. Therefore, the objective of this study was to determine which side, intact or prosthetic, TTAs should carry a load by exploring the effects on gait kinetics. We hypothesized that TTAs would exhibit significant differences in GRF peaks and impulses, loading and unloading rates, loading symmetry, and lower limb kinetics (i.e., moments and powers) while carrying a side load compared to unloaded walking. We also hypothesized that the association between these metrics and loading condition would vary depending on which limb side, intact or prosthetic, the load was carried.

2. Methods

2.1. Human subjects

Twelve unilateral TTAs (Table 1) provided informed consent to participate in a larger protocol approved by the governing institutional review boards. Prior to testing, all subjects were screened to ensure they were moderately active, had used their prosthesis daily for at least six months, and had no self-reported musculoskeletal or gait disorders.

2.2. Instrumentation

All subjects wore a study-provided passive-elastic prosthetic foot (Sierra; Freedom Innovations, Irvine, CA). To add a side load, subjects donned a padded carrier (Ergobaby, Torrance, CA) to carry a cylindrical pack filled with sand for a total added mass of 13.6 kg (30 lbs.). This mass was chosen because it exceeded a 10 kg range, for which an immediate stiffness category change to the study prosthetic foot would be recommended if the additional mass was permanent. Additionally, it simulated a common load carried over one shoulder or hip during walking, such as objects carried in a non-sedentary occupation (>5 kg) (National Bureau of Economic Research, 2016), a toddler (ages 1–2 years) (National Center for Health Statistics, 2021), grocery items, or a sling bag.

Five embedded force plates (AMTI, Watertown, MA) were used to capture three-dimensional GRFs. A 16-camera motion capture system (Vicon Motion Systems, Oxford, UK) recorded marker trajectories at 120 Hz and force plate data at 1,200 Hz. All subjects were provided with tight-fitting clothing to wear during data collection. The same researcher placed 14 mm reflective tracking markers on each subject using Vicon's standard Plug-in-Gait marker configuration, with additional markers placed bilaterally on the medial elbow, medial knee epicondyle, medial malleolus, tibial tuberosity, fibular head, and first and fifth metatarsal heads. Clusters of four markers were also placed bilaterally on the upper arms and thighs. The markers on the prosthetic limb mirrored the intact limb. Lastly, three markers were placed to define the load segment (two on top, one on bottom).

2.3. Experimental protocol

The first study visit was for acclimation and prosthesis fitting. During this study visit, self-selected walking speed was measured over four repeated trials along a 14 m straight hallway while subjects wore their own as-prescribed prosthesis. Subject height, body mass, and anthropometrics were also measured. The study prosthetic foot was then fit and aligned by a certified prosthetist using standard clinical procedures. Subjects walked for up to 15 min to acclimate to each load condition: no load (NL), intact-side load carriage (IL), and prosthetic-side load carriage (PL) (Fig. 1).

For the second study visit, the load conditions were randomized for each subject. Subjects were fit with the study prosthesis, and then reflective markers were placed. Subjects walked at their self-selected speed across the five embedded force plates for a minimum of two repeated trials per condition. Subjects were allowed adequate rest as needed.

Table 1
Subject demographic characteristics, in which body mass includes prosthetic components.

TTA subject	Age (years)	Sex	Body mass (kg)	Height (m)	Amputation etiology	Amputated limb	Residual limb length (mm)	Time since amputation (years)	Study foot stiffness category	Self-selected walking speed (m/s)
1	59	M	83.5	1.67	Trauma	L	130	15	6	1.16
2	40	M	102.3	1.81	Trauma	L	145	10	7	1.67
3	60	M	111.9	1.80	Trauma	R	150	3	7	1.30
4	58	F	96.6	1.69	Congenital	R	190	5	6	1.12
5	39	M	105.7	1.71	Trauma	R	150	12	7	1.43
6	25	F	52.6	1.56	Congenital	R	155	24	2	1.37
7	43	M	107.0	1.82	Infection	L	220	1	7	1.32
8	31	M	98.5	1.83	Trauma	R	[a]	11	7	1.26
9	36	M	110.4	1.86	Trauma	R	200	15	7	1.20
10	29	M	83.9	1.64	Trauma	L	130	3	6	1.16
11	53	M	106.6	1.86	Dysvascular	L	170	7	7	0.92
12	75	M	93.6	1.83	Trauma	L	165	55	7	1.17
Mean (SD)	46 (15)	–	96.1 (16.6)	1.76 (0.10)	–	–	164 (29)	13 (15)	–	1.26 (0.19)

[a] Not measured.

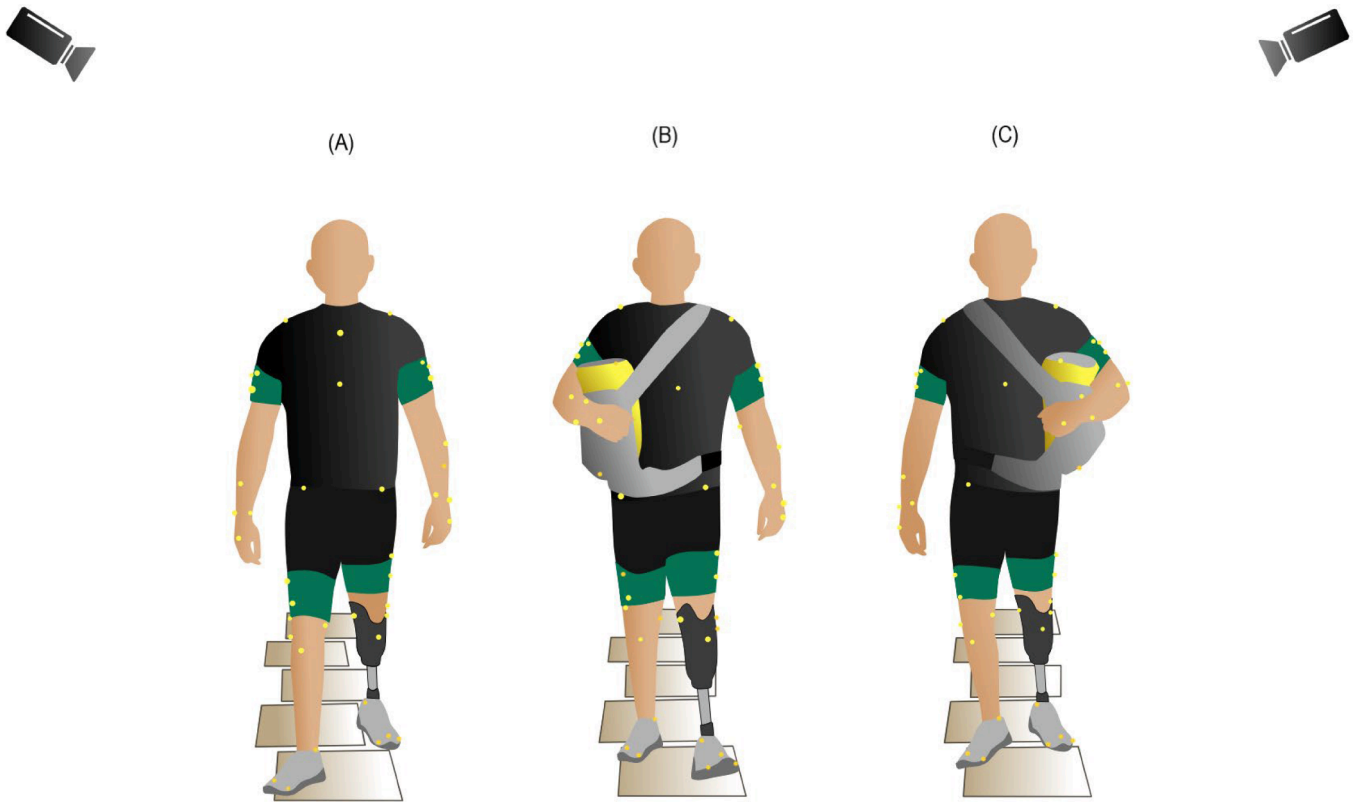

Fig. 1. An illustration of a TTA subject walking overground across five embedded force plates during (A) no load (NL) (B) intact-side load (IL) (C) prosthetic-side load (PL) conditions.

2.4. Data analysis

Raw marker trajectory data were filtered in Vicon Nexus software (Vicon Motion Systems, Oxford, UK) using a Woltring filter with a mean-square-error value of 10 mm^2, based on a fifth-order spline-interpolating function (Woltring, 1986). GRF and lower-limb joint kinetic data were processed and calculated in Visual 3D software (C-Motion, Germantown, USA) with a 15-segment whole-body model (i.e., head, torso, Visual 3D Composite pelvis, and bilateral upper arm, forearm, hand, thigh, shank, and foot; plus, a load segment when applicable). Each segment's mass was estimated as a percentage of whole-body (Dempster, 1995), and the inertial properties and center of mass positions were based on geometric approximations calculated in Visual 3D. The prosthetic shank mass was reduced to 35 % of the intact shank, and the prosthetic center of mass location was moved 35 % closer to the knee joint (Smith et al., 2014). All metrics were calculated for both the intact and prosthetic limbs. Heel strike and toe off events were automatically detected based on a force plate loading threshold of 25 N. These events were also inspected visually, confirming them with kinematic patterns. GRF data included Fx (mediolateral component), Fy (anteroposterior component), and Fz (vertical component). Anterior positive and posterior negative GRF represent propulsive and braking forces, respectively. GRF data were filtered using a digital, fourth order, low-pass Butterworth filter with a cut-off frequency of 25 Hz and normalized by the subject's body mass (kg) for all NL, IL, and PL, including the added side load for IL and PL. Each GRF impulse was determined by time integrating the corresponding GRF component. Loading and unloading rates (Fig. 2) were calculated from vertical GRF (vGRF) curves using a similar method used in other studies (Crowell et al., 2010; Ueda et al., 2016). This method was chosen as it uses the most linear portions of vGRF curves during stance phase. Joint kinetics including hip and knee moments and powers were calculated using inverse dynamics techniques in Visual3D. The joint kinetic profiles were labeled for specific bursts of energy absorption and generation (for powers) and peaks (for moments) (Winter and Sienko, 1988). Ankle power was calculated using the unified deformable segment method (Takahashi et al., 2012). Further data analysis was performed using MATLAB software (The MathWorks Inc., Natick, MA, USA).

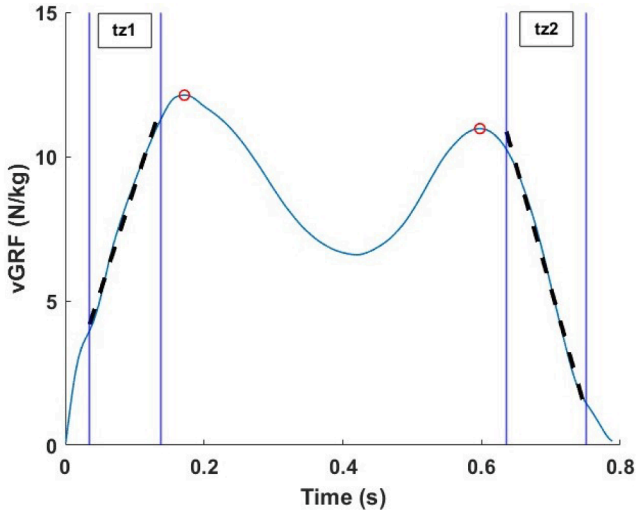

Fig. 2. A representative vertical GRF (vGRF) curve from which loading and unloading rates were calculated. In the figure, tz1: loading period that occurs from heel strike to the first peak vGRF (first red dot), and tz2: unloading period that occurs from the second peak vGRF (second red dot) to toe-off. Loading and unloading rates were estimated as the slope of $vGRF_{max}$ (first black dashed line) over 20–80% time window of tz1 (first blue vertical lines), and as the slope of $vGRF_{max}$ (second black dashed line) over 20–80% time window of tz2 (second blue vertical lines), respectively.

$$\text{Loading rates} = \frac{\Delta \text{vGRF1max}}{\Delta t(20\% < tz1 < 80\%)} \quad (1)$$

$$\text{Unloading rates} = \frac{\Delta \text{vGRF2max}}{\Delta t(20\% < tz2 < 80\%)} \quad (2)$$

Loading symmetry was calculated by estimating the bilateral symmetry index (Cutti et al., 2018), where a value of 1 represents perfect symmetry.

$$\text{vGRF Impulse Symmetry Index} = \frac{\text{vGRF Impulse (intact)}}{\text{vGRF Impulse (prosthetic)}} \quad (3)$$

$$\text{First Peak Symmetry Index} = \frac{\text{first peak vGRF (intact)}}{\text{first peak vGRF (prosthetic)}} \quad (4)$$

Similarly, stance time symmetry (the period in which loading occurred) was also calculated.

2.5. Statistical methods

Linear mixed-effects regression was used to test for an association between each metric (the dependent variable) and load conditions (NL, IL, or PL) for each limb (intact vs. prosthetic), by modeling a load by limb interaction. The load by limb interaction terms allowed estimation of pairwise differences between NL vs. IL, NL vs. PL, and IL vs. PL for each limb. A random intercept for each subject was included to account for overall variability in outcomes across subjects. Random effects were also modeled to allow differences across loads to vary by limb within subject if these estimates could be obtained, otherwise, simpler random effects were modeled. Variance heterogeneity was assessed using plots of residuals against the fitted values, with variance stabilizing transformations of the dependent variable (e.g., logs) considered if necessary. Hypothesis testing was carried out using F-tests for the association between metric and load for each limb, as well as the difference in the association between metric and load by limb by testing for the significance of the load by limb interaction term. The significance of pairwise comparisons between load conditions was assessed using t-tests. The Benjamini-Hochberg correction for multiple testing (Benjamini and Hochberg, 1995) was applied to hypothesis tests for differences in kinetic metrics by limb for each load condition separately, and to interaction effects, to restrict the false discovery rate of the rejected hypotheses to 0.05. A statistical significance level was set at an $\alpha < 0.05$. Pairwise mean differences between load conditions were reported to represent corresponding effect sizes, and 95 % confidence intervals for pairwise comparisons were presented. All statistical analyses were carried out using R 4.3.0 software (R Foundation for Statistical Computing, Vienna, Austria, 2023) and packages tidyverse, lme4 and emmeans.

3. Results

3.1. GRF-related metrics

Within limb comparisons showed that the intact limb had a smaller peak propulsive force in PL compared to NL (pairwise mean difference, p-value [confidence interval]) (0.21 N/kg, $p < 0.01$ [0.06, 0.33]). No strong evidence of associations between load and GRF-related metrics or interaction effects were observed (Table 2 and Fig. 3). Additionally, pairwise comparisons for bilateral loading symmetry showed no significant differences between load conditions (Fig. 4). No change was observed in subjects' self-selected walking speed across load conditions.

3.2. Joint kinetic metrics

For joint power, within limb comparisons revealed a higher intact limb hip extensor power at weight acceptance (HP1) in IL compared to

Table 2
Mean (Standard Error) GRF-related metrics and within limb comparisons for intact and prosthetic limbs. Data are presented and compared according to leading intact and prosthetic limbs. **Bolded** p-values with an asterisk (*) indicate statistical significance (shading for clarity). Pairwise p-values indicate statistical significance for pairwise comparisons between load conditions (NL vs. IL, NL vs. PL, and IL vs. PL). Abbreviations: (NL) no load condition, (IL) intact-side load condition, (PL) prosthetic-side load condition, (GRF) ground reaction force.

Metrics	Units	Mean (Standard Error)							Pairwise p-value [95 % confidence interval]						p-value
		Intact Limb				Prosthetic Limb			Intact Limb			Prosthetic Limb			Interaction (Load*Limb)
		NL	IL	PL	p-value	NL	IL	PL	p-value	NL vs. IL	NL vs. PL	IL vs. PL	NL vs. IL	NL vs. PL	IL vs. PL	
First peak vertical GRF	N/kg	11.74 (0.27)	11.72 (0.30)	11.36 (0.30)	0.21	10.61 (0.27)	10.13 (0.30)	10.74 (0.31)	0.09	0.99 [-0.43, 0.48]	0.09 [-0.05, 0.81]	0.26 [-0.19, 0.90)	**0.03*** **[0.04, 0.91]**	0.76 [-0.60, 0.34]	**0.03*** **[-1.17, −0.04]**	0.13
Peak propulsive force		2.05 (0.15)	1.85 (0.12)	1.84 (0.14)	**0.04***	1.53 (0.15)	1.41 (0.12)	1.39 (0.14)	0.18	0.07 [-0.001, 0.041]	**<0.01*** **[0.06, 0.33]**	0.99 [-0.14,0.13]	0.31 [-0.08,0.33]	0.06 [-0.01,0.27]	0.97 [-0.12,0.14]	0.79
Peak braking force		−1.88 (0.12)	−1.76 (0.13)	−1.94 (0.13)	0.61	−1.22 (0.12)	−1.12 (0.13)	−1.27 (0.14)	0.71	0.69 [-0.47,0.23]	0.91 [-0.28,0.39]	0.47 [-0.19,0.54]	0.75 [-0.45,0.24]	0.94 [-0.32,0.41]	0.59 [-0.23, 0.53]	0.99
Loading rates	N/kg/s	8.03 (0.71)	8.07 (0.73)	7.94 (0.72)	0.97	6.91 (0.72)	6.18 (0.72)	7.52 (0.75)	0.18	1.00 [-1.30, 1.22]	0.98 [-1.13, 1.31]	0.97 [-1.16, 1.42]	0.33 [-0.50, 1.95]	0.50 [-1.93, 0.71]	**0.05*** **[-2.65, −0.01]**	0.43
Unloading rates		−9.00 (0.69)	−8.13 (0.70)	−7.77 (0.69)	0.21	−7.96 (0.69)	−7.80 (0.69)	−7.82 (0.72)	0.97	0.30 [-2.26, 0.53]	0.08 [-2.59, 0.13]	0.81 [-1.76, 1.04]	0.96 [-1.52, 1.20]	0.97 [-1.58, 1.31]	1.00 [-1.43, 1.47]	0.64
Vertical impulse	Ns/kg	5.81 (0.17)	5.80 (0.17)	5.74 (0.16)	0.93	5.26 (0.17)	5.26 (0.17)	5.32 (0.17)	0.90	0.99 [-0.24, 0.27]	0.95 [-0.30, 0.23]	0.88 [-0.27, 0.19]	1.00 [-0.25, 0.25]	0.87 [-0.34, 0.22]	0.82 [-0.30, 0.18]	0.99
Propulsive impulse		0.36 (0.02)	0.34 (0.02)	0.35 (0.02)	0.08	0.24 (0.02)	0.23 (0.02)	0.22 (0.02)	0.34	**0.02*** **[0.00, 0.04]**	0.12 [0.00, 0.03]	0.49 [-0.03, 0.01]	0.53 [-0.01, 0.03]	0.19 [0.00, 0.03]	0.84 [-0.02,0.02]	0.64
Braking impulse		−0.33 (0.02)	−0.33 (0.02)	−0.34 (0.02)	0.93	−0.25 (0.02)	−0.23 (0.02)	−0.25 (0.02)	0.74	0.93 [-0.04, 0.05]	0.87 [-0.03, 0.05]	0.99 [-0.04, 0.05]	0.65 [-0.06, 0.03]	0.99 [-0.05, 0.05]	0.76 [-0.03, 0.06]	0.79
Mediolateral impulse		0.24 (0.04)	0.29 (0.04)	0.24 (0.04)	0.31	0.13 (0.04)	0.19 (0.04)	0.19 (0.04)	0.43	0.49 [-0.16, 0.06]	0.99 [-0.08, 0.09]	0.18 [-0.02, 0.13]	0.42 [-0.16, 0.05]	0.26 [-0.15,0.03]	0.99 [-0.08, 0.07]	0.44

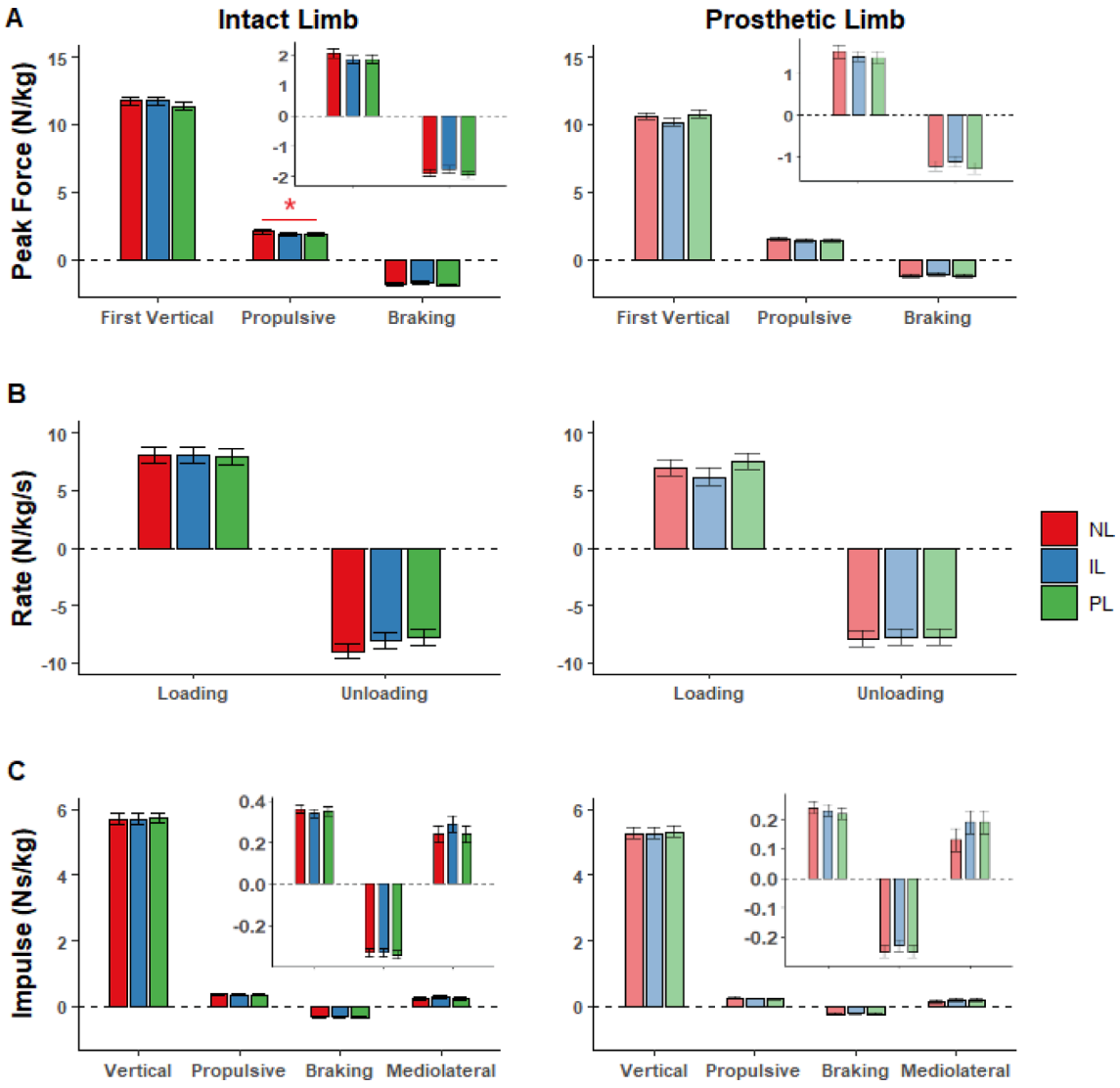

Fig. 3. Within limb comparisons of GRF-related metrics between load conditions for intact limb and prosthetic limb for (A) First peak vGRF, Peak propulsive force, and peak braking force (B) Loading and unloading rates, and (C) Vertical, propulsive, braking, and mediolateral impulses. Asterisk signs represent significant differences between load conditions: (*) indicates $p < 0.05$. NL: no load condition, IL: intact-side load condition, PL: prosthetic-side load condition.

NL (0.32 W/kg, $p < 0.01$ [-0.51, −0.13]). The intact limb also had marginally smaller hip flexor power at push-off (HP3) in PL by 0.18 W/kg compared to NL ($p < 0.01$ [0.1, 0.3]) (Table 3 and Fig. 5). The prosthetic limb had a higher hip extensor power at weight acceptance (HP1) in PL compared to NL (0.39 W/kg, $p < 0.01$ [−0.54, −0.23]). The prosthetic limb also exhibited smaller hip flexor power (HP2) in PL compared to NL (0.19 W/kg, $p < 0.01$ [−0.32, −0.06]). Additionally, the prosthetic limb exhibited smaller hip flexor power at push-off (HP3) in IL by 0.25 W/kg compared to NL ($p < 0.01$ [0.1, 0.4]) (Table 3 and Fig. 5).

Within limb comparisons for sagittal-plane joint moments showed a smaller intact limb hip flexor moment in the stance-swing transition (HM2) in IL (0.18 Nm/kg, $p < 0.01$ [−0.3, −0.06]) and PL (0.16 Nm/kg, $p < 0.01$ [−0.23, −0.08]) compared to NL. The intact limb also had marginally smaller knee flexor moment at the end of swing (KM2) in IL compared to NL (0.07 Nm/kg, $p = 0.01$ [-0.12, −0.01]). The prosthetic limb had smaller hip flexor moment in the stance-swing transition (HM2) in PL by 0.15 Nm/kg compared to NL ($p < 0.01$ [-0.23, −0.07]). (Table 3 and Fig. 6). Within limb comparisons showed differences in most frontal-plane joint moments. The intact limb had higher hip abductor moment in early (HMf1) (0.27 Nm/kg, $p = 0.01$ [-0.45, −0.08]) and late (HMf2) (0.22 Nm/kg, $p < 0.01$ [-0.34, −0.11]) stance in PL compared to NL. Knee abductor moment in early (KMf1) and late (KMf2) stance was also higher by 0.1 Nm/kg ($p = 0.01$ [-0.16, −0.02]) and 0.06 Nm/kg ($p = 0.05$ [-0.12, −0.00]), respectively, in PL compared to NL. Similarly, the prosthetic limb had 0.14 Nm/kg higher hip abductor moment in early stance (HMf1) ($p = 0.02$ [-0.26, −0.02]) and 0.14 Nm/kg higher hip abductor moment in late stance (HMf2) ($p < 0.01$ [-0.23, −0.05]) in IL compared to NL. Additionally, knee abductor moment in early (KMf1) and late (KMf2) stance were higher in IL compared to NL (0.08 Nm/kg, $p = 0.03$ [-0.15, −0.01] and $p < 0.01$ [-0.14, −0.03], respectively) (Table 3 and Fig. 6). All other joint kinetic metrics were not different across load conditions, and no strong evidence of associations between load and these other metrics were observed (Table 3).

A significant interaction effect ($p < 0.01$) was observed for hip extensor power at weight acceptance (HP1) due to the higher hip power generation associated with the limb that carried the load. Significant interactions were also observed for hip abductor moment in early (HMf1) and late (HMf2) stance, and knee abductor moment in early (KMf1) and late (KMf2) stance due to the higher abductor moment on the contralateral limb with respect to the load side (Table 3).

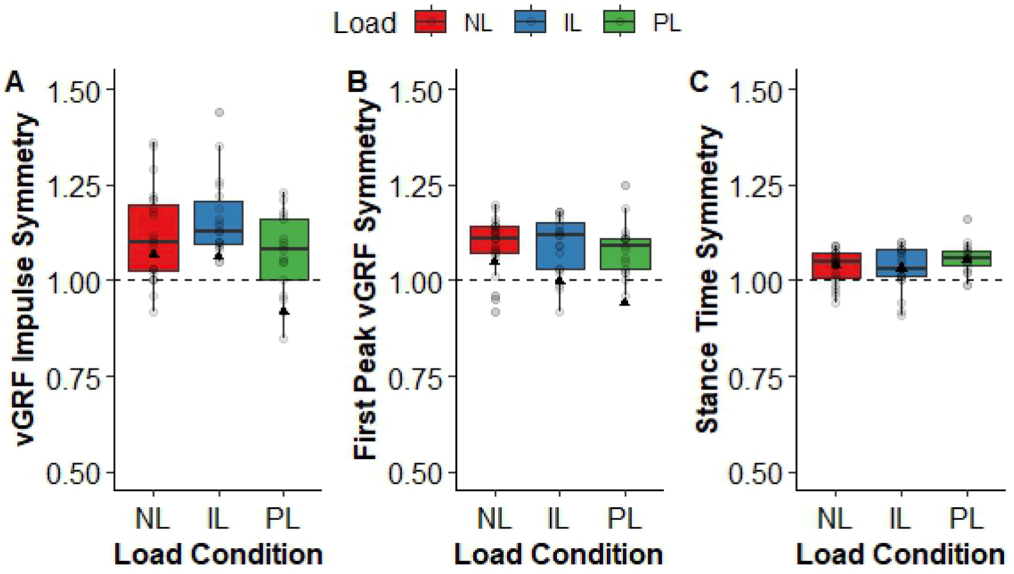

Fig. 4. Pairwise comparisons between load conditions for loading symmetry index of (A) Vertical impulse and (B) First peak vGRF, and for temporal symmetry index of (C) Stance time. Black triangles represent mean values and dash lines at y-axis = 1 represent perfect bilateral symmetry. Asterisk signs represent significant differences between load conditions: (*) indicates $p < 0.05$. NL: no load condition, IL: intact-side load condition, PL: prosthetic-side load condition.

To supplement our findings for kinetic metrics, a figure showing the intact and prosthetic hip and knee angles during NL, IL, and PL conditions is provided in the Supplementary Material. Consistent with the kinetic results, the intact and prosthetic hip and knee kinematics during no load and loaded conditions demonstrate less variability in the sagittal plane than the frontal plane (see Fig. S1).

4. Discussion

The objective of this study was to determine which side, intact or prosthetic, TTAs should carry a load by exploring loading effects on their gait kinetics. TTAs were found to have a smaller peak propulsive force on their intact limb while carrying a load on their prosthetic side, compared to unloaded walking. The activity of ankle plantarflexors (i.e., gastrocnemius and soleus) may explain this effect. Previous research has shown that these muscles act to rotate the body towards the contralateral side and provide frontal plane balance control in late stance (Neptune and McGowan, 2016). With the added contralateral load, the ankle plantarflexor activity would need to decrease rotating the body towards the swinging (prosthetic) limb that is further assisted by gravity, leading to smaller propulsion.

Findings from joint powers showed that TTAs had a higher hip extensor power generation at weight acceptance on the limb carrying the load, compared to unloaded walking. They also had a smaller power generated by hip flexors at push-off in the opposite-side load condition. When the load was carried on the prosthetic side, TTA subjects had a smaller power absorbed by hip flexors on the prosthetic limb compared to unloaded walking. These results suggest that higher hip extensor power generation and smaller hip flexor power absorption are observed on the loaded limb. A significant interaction effect for powers indicates that the higher extensor power generation at weight acceptance was associated with the ipsilateral side load. The hip muscles are known to be important contributors to the dynamic balance of the head-arms-trunk segment. For example, adductor magnus and hamstring muscles act similar to plantarflexors in controlling frontal plane balance (Neptune and McGowan, 2016). During early stance, the activity of the biarticular hamstrings would rotate the body toward the contralateral limb, generating higher hip extensor power on the ipsilateral limb with the added load. By contrast, other studies demonstrate smaller hip extensor power generation at weight acceptance on both limbs when TTAs walk with a back load (Doyle et al., 2014), suggesting that kinetic response at the hip may vary depending on the location of the added load.

TTAs had a smaller hip flexor moment in the stance-swing transition on their intact limb during side loaded conditions compared to unloaded condition. Further, they had 23 % smaller knee flexor moment on their intact limb at the end of swing during the intact-side load condition compared to the prosthetic-side loaded and unloaded conditions. This phenomenon may be explained by prolonged activity in the ipsilateral vastus lateralis throughout swing phase, observed in non-amputee individuals carrying hand-held and back loads (20–50 % body mass) (Ghori and Luckwill, 1985). Significant prolongation of the knee extensors activity to increase body support for the extra load may contribute to the decrease in knee flexor moment. A similar trend was also observed in TTA walking with a back load as they reduced knee flexor moment by 20 % on their prosthetic limb compared to no load condition (Doyle et al., 2014). A surprising result was the absence of a knee extensor response with the added loads. Prior research has shown that the knee extensors act to rotate the body towards the swing leg (Neptune and McGowan, 2016). However, with the added load comes an increased demand for body support, provided by the knee extensors. Thus, it appears the intact hip abductor moment was sufficient to offset the rotation caused by the intact side load.

A significant interaction for moments showed that hip abductor moments on the intact limb and prosthetic limb increased the most in early and late stance during the prosthetic side and intact side load conditions, respectively. These findings are consistent with previous work suggesting that a contralateral load requires higher hip abductor activity on the ipsilateral side due to higher internal torque demand (Neumann et al., 1992; Neumann and Hase, 1994), and that hip abductor (gluteus medius) is a primary contributor to body support and a regulator of frontal plane balance control that acts to rotate the body towards the ipsilateral limb (Neptune and McGowan, 2016) to counteract the added side load.

Certain limitations should be acknowledged while interpreting these results. First, these data are from a relatively small sample of mostly male, traumatic TTAs. While statistical significance was found for some outcome metrics, more subjects would be needed to generalize these results to a larger TTA population, including those with diabetic/dysvascular etiology (for whom load carriage may induce fatigue). These

Table 3
Mean (Standard Error) sagittal peak joint power, sagittal and frontal peak joint moment metrics and within limb comparisons for intact and prosthetic limbs. Data are presented and compared according to leading intact and prosthetic limbs. **Bolded** p-values with an asterisk (*) indicate statistical significance (shading for clarity). Pairwise p-values indicate statistical significance for pairwise comparisons between load conditions (NL vs. IL, NL vs. PL, and IL vs. PL). Abbreviations: (NL) no load condition, (IL) intact-side load condition, (PL) prosthetic-side load condition, (HP) hip power, (KP) knee power, (AP) ankle power, (HM) hip moment, (KM) knee moment.

Metrics	Units	Mean (Standard Error)								Pairwise p-value [95 % confidence interval]						p-value
		Intact Limb				Prosthetic Limb				Intact Limb			Prosthetic Limb			Interaction (Load*Limb)
		NL	IL	PL	p-value	NL	IL	PL	p-value	NL vs. IL	NL vs. PL	IL vs. PL	NL vs. IL	NL vs. PL	IL vs. PL	
Sagittal Power																
HP1 (generation)	W/kg	0.35 (0.1)	0.68 (0.1)	0.36 (0.1)	**0.01***	0.67 (0.1)	0.51 (0.1)	1.06 (0.1)	**<0.01***	**<0.01* [-0.51, −0.13]**	1 [-0.14, 0.14]	**0.02* [0.1, 0.6]**	0.08 [-0.02, 0.34]	**<0.01* [-0.54, −0.23]**	**<0.01* [-0.8, −0.3]**	**<0.01***
HP2 (absorption)		−0.39 (0.08)	−0.27 (0.06)	−0.31 (0.05)	0.3	−0.5 (0.08)	−0.36 (0.06)	−0.31 (0.06)	**0.04***	0.17 [-0.29, 0.04]	0.26 [-0.21, 0.04]	0.7 [-0.1, 0.2]	0.11 [-0.29, 0.02]	**<0.01* [-0.32, −0.06]**	0.54 [-0.2, 0.1]	0.48
HP3 (generation)		0.83 (0.1)	0.83 (0.1)	0.65 (0.1)	**0.05***	0.88 (0.1)	0.64 (0.1)	0.83 (0.1)	**0.01***	1 [-0.2, 0.2]	**<0.01* [0.1, 0.3]**	0.08 [-0.02, 0.39]	**<0.01* [0.1, 0.4]**	0.68 [-0.1, 0.2]	0.05 [-0.4, 0.0]	0.11
KP1 (absorption)		−1.1 (0.15)	−1.09 (0.16)	−0.89 (0.15)	0.18	−0.35 (0.15)	−0.29 (0.15)	−0.45 (0.16)	0.43	−0.99 [-0.26, 0.23]	0.08 [-0.44, 0.02]	0.14 [-0.4, 0.1]	0.82 [-0.28, 0.17]	0.59 [-0.15, 0.34]	0.27 [-0.1, 0.4]	0.19
KP2 (generation)		0.75 (0.08)	0.59 (0.09)	0.58 (0.08)	0.22	0.24 (0.08)	0.09 (0.08)	0.16 (0.09)	0.34	0.18 [-0.05, 0.37]	0.11 [-0.03, 0.38]	0.98 [-0.2, 0.2]	0.17 [-0.05, 0.35]	0.61 [-0.13, 0.29]	0.71 [-0.3, 0.1]	0.82
KP3 (absorption)		−0.97 (0.16)	−1.05 (0.19)	−1.07 (0.14)	0.43	−1.06 (0.16)	−1.17 (0.19)	−1.05 (0.14)	0.56	0.73 [-0.2, 0.4]	0.31 [-0.1, 0.3]	0.99 [-0.3, 0.3]	0.48 [-0.1, 0.4]	0.97 [-0.2, 0.2]	0.46 [-0.4, 0.1]	0.68
KP4 (absorption)		−1.26 (0.09)	−1.16 (0.09)	−1.29 (0.09)	0.25	−0.94 (0.09)	−0.88 (0.09)	−0.83 (0.09)	0.34	0.26 [-0.26, 0.05]	0.87 [-0.12, 0.18]	0.11 [-0.02, 0.29]	0.54 [-0.21, 0.08]	0.18 [-0.27, 0.04]	0.7 [-0.2, 0.1]	0.36
AP1 (absorption)		−0.99 (0.09)	−1.03 (0.1)	−1.05 (0.09)	0.81	−1.21 (0.09)	−1.14 (0.09)	−1.31 (0.1)	0.34	0.93 [-0.2, 0.3]	0.8 [-0.2, 0.3]	0.97 [-0.2, 0.25]	0.69 [-0.3, 0.1]	0.49 [-0.1, 0.3]	0.14 [-0.1, 0.4]	0.68
AP2 (generation)		2.61 (0.23)	2.57 (0.24)	2.41 (0.23)	0.25	1.64 (0.23)	1.62 (0.23)	1.61 (0.24)	0.99	0.92 [-0.2, 0.3]	0.13 [-0.1, 0.5]	0.31 [-0.1, 0.4]	0.99 [-0.2, 0.3]	0.97 [-0.2, 0.3]	0.99 [-0.2, 0.3]	0.68
Sagittal Moment																
HM1 (extension)	Nm/kg	0.45 (0.06)	0.49 (0.06)	0.47 (0.09)	0.61	0.49 (0.06)	0.5 (0.06)	0.56 (0.09)	0.56	0.47 [-0.11, 0.04]	0.93 [-0.14, 0.11]	0.93 [-0.1, 0.2]	0.97 [-0.08, 0.07]	0.42 [-0.2, 0.07]	0.52 [-0.2, 0.1]	0.72
HM2 (flexion)		−0.7 (0.07)	−0.52 (0.06)	−0.55 (0.07)	**<0.01***	−0.7 (0.07)	−0.6 (0.06)	−0.55 (0.07)	**<0.01***	**<0.01* [-0.3, −0.06]**	**<0.01* [-0.23, −0.08]**	0.75 [-0.1, 0.1]	0.11 [-0.21, 0.02]	**<0.01* [-0.23, −0.07]**	0.29 [-0.13, 0.03]	0.56
HM3 (extension)		0.4 (0.04)	0.36 (0.04)	0.4 (0.04)	0.43	0.38 (0.04)	0.33 (0.04)	0.3 (0.04)	0.08	0.31 [-0.03, 0.12]	0.99 [-0.07, 0.08]	0.39 [-0.12, 0.03]	0.17 [-0.02, 0.12]	**0.02* [0.01, 0.16]**	0.47 [-0.03, 0.1]	0.36
KM1 (extension)		0.89 (0.06)	0.81 (0.07)	0.77 (0.06)	0.12	0.43 (0.06)	0.36 (0.06)	0.43 (0.07)	0.34	0.2 [-0.03, 0.2]	**0.03* [0.01, 0.23]**	0.74 [-0.08, 0.15]	0.25 [-0.04, 0.18]	1 [-0.11, 0.12]	0.31 [-0.18, 0.04]	0.48
KM2 (flexion)		−0.31 (0.02)	−0.24 (0.02)	−0.3 (0.02)	**0.05***	−0.27 (0.02)	−0.23 (0.02)	−0.22 (0.02)	0.18	**0.01* [-0.12, −0.01]**	0.85 [-0.06, 0.04]	**0.04* [0.00, 0.11]**	0.15 [-0.09, 0.01]	0.08 [-0.1, 0.01]	0.9 [-0.06, 0.04]	0.36
Frontal Moment																
HMf1 (abduction)	Nm/kg	0.91 (0.07)	0.60 (0.06)	1.18 (0.05)	**<0.01***	0.74 (0.07)	0.88 (0.06)	0.39 (0.05)	**<0.01***	**<0.01* [0.18, 0.44]**	**0.01* [-0.45, −0.08]**	**<0.01* [-0.72, −0.43]**	**0.02* [-0.26, −0.02]**	**<0.01* [0.16, 0.54]**	**<0.01* [0.35, 0.64]**	**<0.01***
HMf2 (abduction)		0.72 (0.06)	0.47 (0.05)	0.94 (0.04)	**<0.01***	0.67 (0.06)	0.81 (0.05)	0.39 (0.05)	**<0.01***	**<0.01* [0.15, 0.35]**	**<0.01* [-0.34, −0.11]**	**<0.01* [-0.58, −0.37]**	**<0.01* [-0.23, −0.05]**	**<0.01* [0.17, 0.42]**	**<0.01* [0.33, 0.54]**	**<0.01***
KMf1 (abduction)		0.36 (0.03)	0.25 (0.04)	0.46 (0.03)	**<0.01***	0.23 (0.03)	0.31 (0.03)	0.14 (0.04)	**<0.01***	**<0.01* [0.04, 0.19]**	**0.01* [-0.16, −0.02]**	**<0.01* [-0.28, −0.13]**	**0.03* [-0.15, −0.01]**	**0.01* [0.02, 0.17]**	**<0.01* [0.10, 0.25]**	**<0.01***
KMf2 (abduction)		0.31 (0.03)	0.24 (0.03)	0.37 (0.03)	**<0.01***	0.12 (0.03)	0.20 (0.03)	0.09 (0.03)	**<0.01***	**0.01* [0.02, 0.12]**	**0.05* [-0.12, −0.00]**	**<0.01 [-0.18, −0.08]**	**<0.01* [-0.14, −0.03]**	0.57 [-0.04, 0.09]	**<0.01* [0.05, 0.17]**	**<0.01***

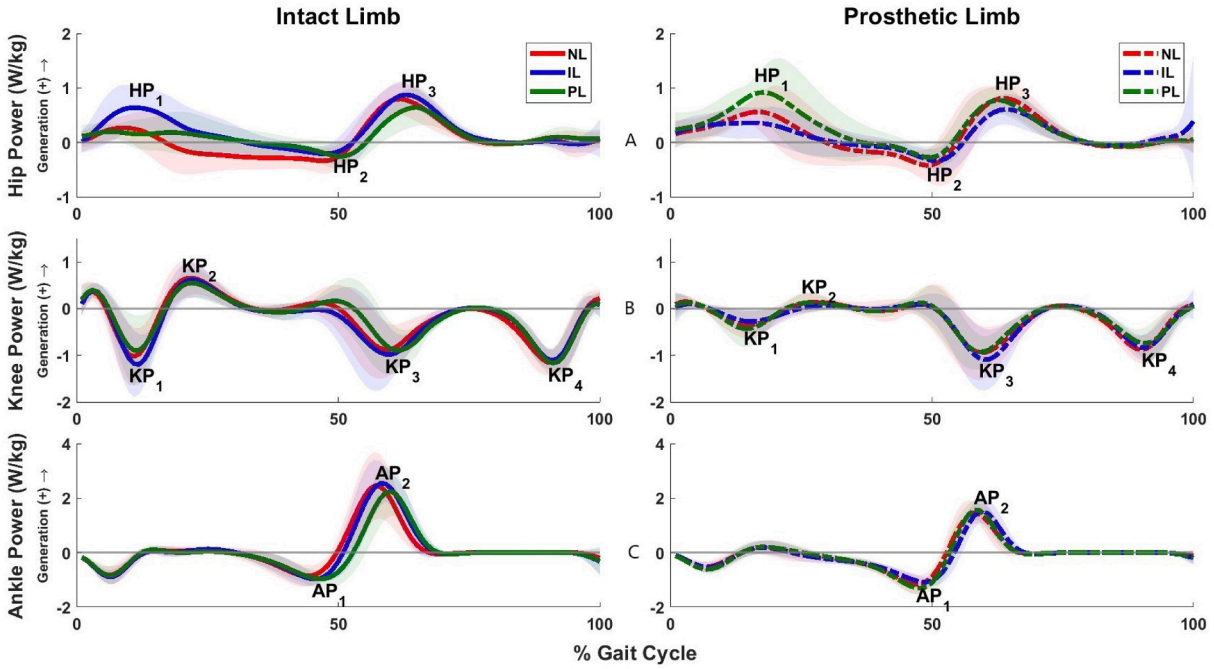

Fig. 5. Mean sagittal joint power profiles at the (A) hip, (B) knee, and (C) ankle for the intact (solid lines) and prosthetic (dashed lines) limbs in NL, IL, and PL. Power generation indicating concentric muscle contraction is positive. NL: no load condition, IL: intact-side load condition, PL: prosthetic-side load condition.

results may not generalize to transfemoral amputees who adopt different gait compensatory strategies (Varrecchia et al., 2019) due to greater musculoskeletal loss. For instance, those with osseointegrated prostheses have improved static balance (Gaffney et al., 2023) but maintain loading asymmetry (Thomsen et al., 2024). Second, we used an added load that exceeded the 10 kg range for which an immediate change to a stiffer prosthetic foot would be recommended, and to simulate a typical side load carried by individuals with and without TTA in daily activities. However, this load was not as heavy as those reported by other studies in individuals without amputation (Wang et al., 2012) and TTAs (Doyle et al., 2015, 2014). Higher loads (e.g., >20 % body mass) that are typically required for military activities may yield more significant differences in GRF parameters. Next, we only included a passive elastic prosthetic foot in the analysis of this current study. This foot was selected to reflect the standard-of-care feet. This is a realistic scenario in which most TTAs do not have adapting feet, and this is what they would experience in their daily lives. Further, we selected this foot to avoid potential confounds due to differing prosthetic systems and foot designs that may influence GRF (Snyder et al., 1995). However, we acknowledge that the constant stiffness characteristics of the study prosthetic foot represent a substantial limitation in functionality. There could be potential benefits of a more versatile prosthetic foot design for load carriage applications that were not explored here. Additionally, while we discussed the kinetic changes in this study in light of the biomechanical activity of relevant muscles, we did not collect EMG data to support our arguments and confirm these results. Future work should include EMG observations to confirm these discussions.

This study provides insight into certain gait kinetics for TTAs walking overground during side load carriage conditions. While the results may provide some evidence to support our hypotheses, our study demonstrated mixed findings to determine which side TTAs should carry a load, suggesting that it depends on the desired kinetic effects, particularly on their intact limb. For example, the intact limb propulsive force would be smaller if the load were carried on the prosthetic side, suggesting two clinical implications. First, it may reduce the demand on ankle plantarflexors, which can benefit individuals, including TTAs, who have muscle weakness by reducing mechanical strain during loaded walking. Second, the decreased intact limb propulsion may potentially lead to inefficient gait and compensatory patterns over time. To address this, rehabilitation strategies associated with prosthetic-side load carriage could focus on physical therapy to strengthen key muscle contributors to forward propulsion (e.g., intact-side gastrocnemius and soleus) (Liu et al., 2006; Neptune et al., 2004, 2001) and balance control (e.g., vasti, gluteus medius) (Neptune and McGowan, 2016). In contrast to prosthetic-side load condition, the intact hip flexor moment in late stance and knee flexor moment in late swing would be slightly smaller if TTAs carried their load on the intact side. This finding may compromise balance control by increasing the risk of insufficient foot clearance on their intact limb. The decrease in hip and knee flexor moments can lead to a higher likelihood of tripping, which may be mitigated with rehabilitation strategies such as muscle strengthening (e.g., for intact-side iliopsoas, hamstrings, and gastrocnemius) and balance training. Further, targeted prosthetic gait training could improve load distribution across both limbs and enhance walking coordination during load carriage activities. However, further study is warranted to investigate if these effects are substantial when carrying a side load over time. Additionally, future work may increase the mass of side load to reflect more heavy-duty activities, for which a stiffer prosthetic foot or one purported for sudden increased loading (e.g., powered foot, foot with heel-stiffening wedge or dual keel) is recommended. If the effects are indeed clinically significant, prosthetic designs, as well as gait rehabilitation for TTAs who routinely carry a side load, should take these results into consideration.

CRediT authorship contribution statement

Satria Ardianuari: Writing – review & editing, Writing – original draft, Visualization, Software, Methodology, Investigation, Formal analysis, Conceptualization. **Krista M. Cyr:** Writing – review & editing, Software, Investigation, Formal analysis. **Richard R. Neptune:** Writing – review & editing, Project administration, Investigation, Funding acquisition, Conceptualization. **Glenn K. Klute:** Writing – review & editing, Supervision, Resources, Project administration, Methodology, Funding acquisition, Conceptualization.

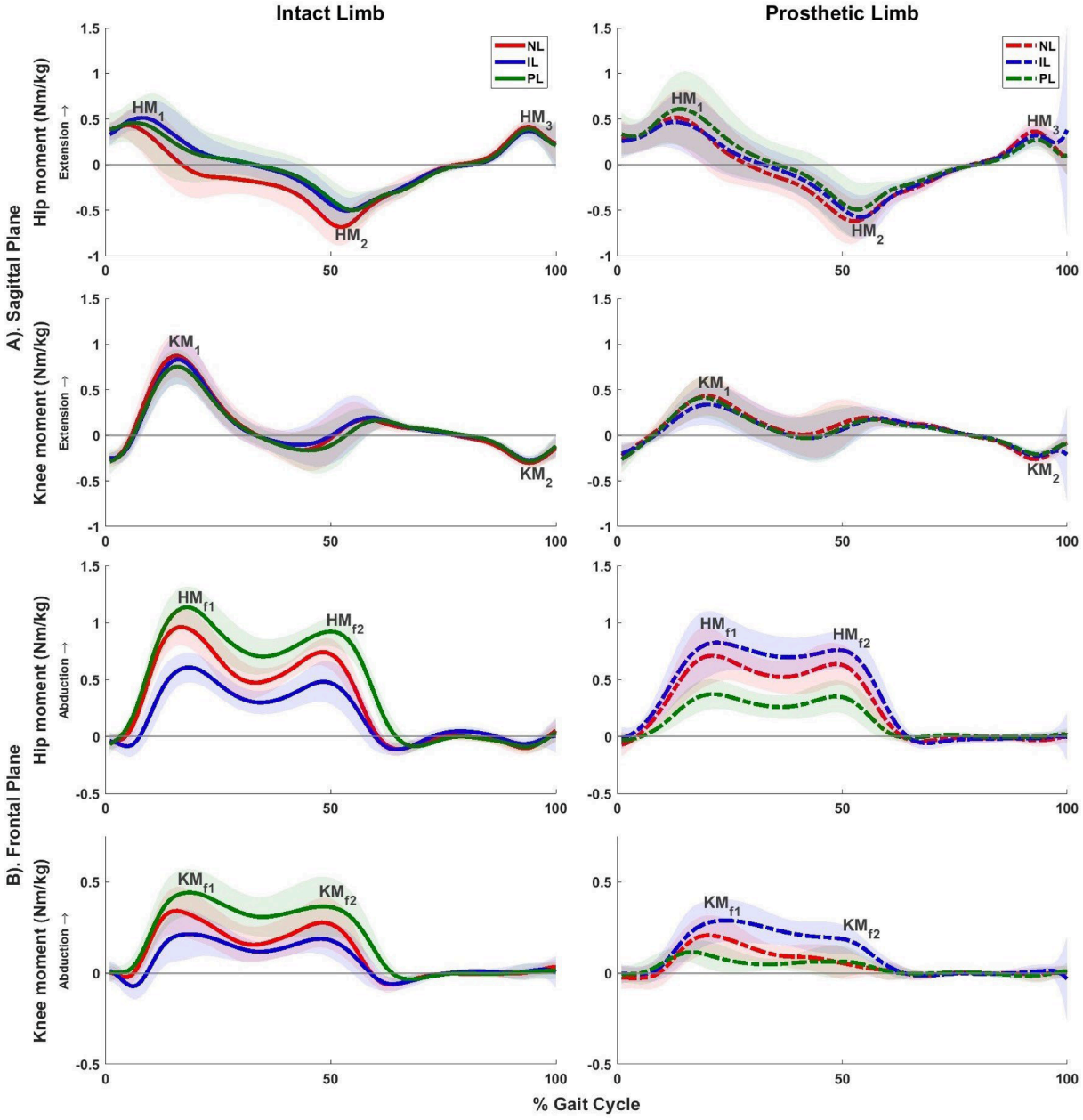

Fig. 6. A). Mean sagittal internal joint moments and B). Mean frontal internal joint moments at the hip and knee for the intact (solid lines) and prosthetic (dashed lines) limbs in NL, IL, and PL. Extensor and abductor moments are positive. NL: no load condition, IL: intact-side load condition, PL: prosthetic-side load condition.

Declaration of competing interest

The authors declare that they have no known competing financial interests or personal relationships that could have appeared to influence the work reported in this paper.

Acknowledgments

Christina Carranza, L/CPO (licensed/certified prosthetist) fit and aligned the study prosthesis for all TTA subjects, and Jane Shofer, MS (biostatistician) provided consulting for the statistical analyses.

This work was supported in part by Merit Review Award Number I01 RX003138 and by Career Development/Capacity Building Award Number IK6 RX002974 from the United States Department of Veterans Affairs Rehabilitation Research and Development Service, and through the 2022 Fellowship funds from the Orthotic and Prosthetic Education and Research Foundation, Inc.

Appendix A. Supplementary data

Supplementary data to this article can be found online at https://doi.org/10.1016/j.jbiomech.2024.112385.

References

Anderson, F.C., Pandy, M.G., 2003. Individual muscle contributions to support in normal walking. Gait Posture 17, 159–169.

Attwells, R.L., Birrell, S.A., Hooper, R.H., Mansfield, N.J., 2006. Influence of carrying heavy loads on soldiers' posture, movements and gait. Ergonomics 49, 1527–1537. https://doi.org/10.1080/00140130600757237.

Bateni, H., Olney, S.J., 2002. Kinematic and kinetic variations of below-knee amputee gait. Journal of Prosthetics and Orthotics 14.

Benjamini, Y., Hochberg, Y., 1995. Controlling the False Discovery Rate: A Practical and Powerful Approach to Multiple Testing, Source: Journal of the Royal Statistical Society. Series B. Methodological.

Birrell, S.A., Haslam, R.A., 2009. The effect of military load carriage on 3-D lower limb kinematics and spatiotemporal parameters. Ergonomics 52, 1298–1304. https://doi.org/10.1080/00140130903003115.

Burke, M.J., Roman, V., Wright, V., 1978. Bone and joint changes in lower limb amputees. Annals of the Rheumatic Diseases.
Crowell, H.P., Milnert, C.E., Hamill, J., Davis, I.S., 2010. Reducing impact loading during running with the use of real-time visual feedback. Journal of Orthopaedic and Sports Physical Therapy 40, 206–213. https://doi.org/10.2519/jospt.2010.3166.
Cutti, A.G., Verni, G., Migliore, G.L., Amoresano, A., Raggi, M., 2018. Reference values for gait temporal and loading symmetry of lower-limb amputees can help in refocusing rehabilitation targets. J Neuroeng Rehabil 15. https://doi.org/10.1186/s12984-018-0403-x.
Dean, J.C., Alexander, N.B., Kuo, A.D., 2007. The effect of lateral stabilization on walking in young and old adults. IEEE Trans Biomed Eng 54, 1919–1926. https://doi.org/10.1109/TBME.2007.901031.
Dempster, W.T., 1995. Space requirements of the seated operator : geometrical, kinematic, and mechanical aspects of the body, with special reference to the limbs. WADC Technical Report 55–159.
Doyle, S.S., Lemaire, E.D., Besemann, M., Dudek, N.L., 2014. Changes to level ground transtibial amputee gait with a weighted backpack. Clinical Biomechanics 29, 149–154. https://doi.org/10.1016/j.clinbiomech.2013.11.019.
Doyle, S.S., Lemaire, E.D., Besemann, M., Dudek, N.L., 2015. Changes to transtibial amputee gait with a weighted backpack on multiple surfaces. Clinical Biomechanics 30, 1119–1124. https://doi.org/10.1016/j.clinbiomech.2015.08.015.
Gaffney, B.M.M., Davis-Wilson, H.C., Christiansen, C.L., Awad, M.E., Lev, G., Tracy, J., Stoneback, J.W., 2023. Osseointegrated prostheses improve balance and balance confidence in individuals with unilateral transfemoral limb loss. Gait Posture 100, 132–138. https://doi.org/10.1016/J.GAITPOST.2022.12.011.
Gailey, R., Allen, K., Castles, J., Kucharik, J., Roeder, M., 2008. Review of secondary physical conditions associated with lower-limb amputation and long-term prosthesis use. J Rehabil Res Dev 45, 15–30. https://doi.org/10.1682/JRRD.2006.11.0147.
Ghori, G.M.U., Luckwill, R.G., 1985. Responses of the lower limb to load carrying in walking man. Eur J Appl Physiol Occup Physiol 54, 145–150.
Gitter, A., Czerniecki, J., DeGroot, D.M., 1991. Biomechanical analysis of the influence of prosthetic feet on below-knee amputee walking. Am J Phys Med Rehabil 70, 142–148.
Grumillier, C., Martinet, N., Paysant, J., André, J.M., Beyaert, C., 2008. Compensatory mechanism involving the hip joint of the intact limb during gait in unilateral transtibial amputees. J Biomech 41, 2926–2931. https://doi.org/10.1016/j.jbiomech.2008.07.018.
Harman, E., Han, H.-H., Frykman, P., Johnson, M., Russell, F., Rosenstein, M., 1992. The Effects on Gait Timing, Kinetics, and Muscle Activity of Various Loads Carried on The Back. Med Sci Sports Exerc.
Highsmith, M.J., Goff, L.M., Lewandowski, A.L., Farrokhi, S., Hendershot, B.D., Hill, O. T., Rábago, C.A., Russell-Esposito, E., Orriola, J.J., Mayer, J.M., 2019. Low back pain in persons with lower extremity amputation: a systematic review of the literature. Spine Journal 19, 552–563. https://doi.org/10.1016/j.spinee.2018.08.011.
Liu, M.Q., Anderson, F.C., Pandy, M.G., Delp, S.L., 2006. Muscles that support the body also modulate forward progression during walking. J Biomech 39, 2623–2630. https://doi.org/10.1016/j.jbiomech.2005.08.017.
McAndrew, P.M., Wilken, J.M., Dingwell, J.B., 2011. Dynamic stability of human walking in visually and mechanically destabilizing environments. J Biomech 44, 644–649. https://doi.org/10.1016/j.jbiomech.2010.11.007.
National Bureau of Economic Research, 2016. The Requirements of Jobs: Evidence from a Nationally Representative Survey. Cambridge, MA.
National Center for Health Statistics, 2021. Anthropometric Reference Data for Children and Adults: United States, 2015-2018.
Neptune, R.R., McGowan, C.P., 2011. Muscle contributions to whole-body sagittal plane angular momentum during walking. J Biomech 44, 6–12. https://doi.org/10.1016/j.jbiomech.2010.08.015.
Neptune, R.R., McGowan, C.P., 2016. Muscle contributions to frontal plane angular momentum during walking. J Biomech 49, 2975–2981. https://doi.org/10.1016/j.jbiomech.2016.07.016.
Neptune, R.R., Kautz, S.A., Zajac, F.E., 2001. Contributions of the individual ankle plantar flexors to support, forward progression and swing initiation during walking. Journal of. Biomechanics.
Neptune, R.R., Zajac, F.E., Kautz, S.A., 2004. Muscle force redistributes segmental power for body progression during walking. Gait Posture 19, 194–205. https://doi.org/10.1016/S0966-6362(03)00062-6.
Neumann, D.A., Cook, T.M., Sholty, R.L., Sobush, D.C., 1992. An Electromyographic Analysis of Hip Abductor Muscle Activity When Subjects Are Carrying Loads in One or Both Hands. Phys Ther 72, 207–217. https://doi.org/10.1093/PTJ/72.3.207.
Neumann, D.A., Hase, A.D., 1994. An Electromyographic Analysis of the Hip Abductors During Load Carriage: Implications for Hip Joint Protection 19, 296–304. https://doi.org/10.2519/JOSPT.1994.19.5.296.
Nolan, L., Wit, A., Dudziñ, K., Lees, A., Lake, M., Wychowañ, M., 2003. Adjustments in gait symmetry with walking speed in trans-femoral and trans-tibial amputees. Gait Posture 17, 142–151.
Norvell, D.C., Czerniecki, J.M., Reiber, G.E., Maynard, C., Pecoraro, J.A., Weiss, N.S., 2005. The prevalence of knee pain and symptomatic knee osteoarthritis among veteran traumatic amputees and nonamputees. Arch Phys Med Rehabil 86, 487–493. https://doi.org/10.1016/j.apmr.2004.04.034.
Sadeghi, H., Allard, P., Duhaime, M., Hospital, J., 2001. Muscle Power Compensatory Mechanisms in Below-Knee Amputee Gait. Am J Phys Med Rehabil 80, 25–32.
Schnall, B.L., Wolf, E.J., Bell, J.C., Gambel, J., Bensel, C.K., 2012. Metabolic analysis of male servicemembers with transtibial amputations carrying military loads. J Rehabil Res Dev 49, 535–544. https://doi.org/10.1682/JRRD.2011.04.0075.
Schnall, B.L., Hendershot, B.D., Bell, J.C., Wolf, E.J., 2014. Kinematic analysis of males with transtibial amputation carrying military loads. J Rehabil Res Dev 51, 1505–1514. https://doi.org/10.1682/JRRD.2014.01.0022.
Silder, A., Delp, S.L., Besier, T., 2013. Men and women adopt similar walking mechanics and muscle activation patterns during load carriage. J Biomech 46, 2522–2528. https://doi.org/10.1016/j.jbiomech.2013.06.020.
Silverman, A.K., Fey, N.P., Portillo, A., Walden, J.G., Bosker, G., Neptune, R.R., 2008. Compensatory mechanisms in below-knee amputee gait in response to increasing steady-state walking speeds. Gait Posture 28, 602–609. https://doi.org/10.1016/j.gaitpost.2008.04.005.
Smith, J.D., Ferris, A.E., Heise, G.D., Hinrichs, R.N., Martin, P.E., 2014. Oscillation and reaction board techniques for estimating inertial properties of a below-knee prosthesis. Journal of Visualized Experiments. https://doi.org/10.3791/50977.
Snyder, R.D., Powers, C.M., Fontaine, C., Perry, J., 1995. The effect of five prosthetic feet on the gait and loading of the sound limb in dysvascular below-knee amputees. J Rehabil Res Dev 32, 309–315.
Struyf, P.A., van Heugten, C.M., Hitters, M.W., Smeets, R.J., 2009. The Prevalence of Osteoarthritis of the Intact Hip and Knee Among Traumatic Leg Amputees. Arch Phys Med Rehabil 90, 440–446. https://doi.org/10.1016/j.apmr.2008.08.220.
Takahashi, K.Z., Kepple, T.M., Stanhope, S.J., 2012. A unified deformable (UD) segment model for quantifying total power of anatomical and prosthetic below-knee structures during stance in gait. J Biomech 45, 2662–2667. https://doi.org/10.1016/j.jbiomech.2012.08.017.
Templin, T.N., Klute, G.K., Neptune, R.R., 2021. The influence of load carriage on knee joint loading and metabolic cost on walking with lower-limb amputation: a preliminary modeling study. Journal of Prosthetics and Orthotics 33.
Thomsen, P.B., Gaffney, B.M.M., Tracy, J.B., Vandenberg, N.W., Awad, M.E., Christiansen, C.L., Stoneback, J.W., 2024. Cumulative loading increases and loading asymmetries persist during walking for people with a transfemoral bone-anchored limb. Gait Posture 113, 46–52. https://doi.org/10.1016/J.GAITPOST.2024.05.019.
Ueda, T., Hobara, H., Kobayashi, Y., Heldoorn, T.A., Mochimaru, M., Mizoguchi, H., 2016. Comparison of 3 methods for computing loading rate during running. Int J Sports Med 37, 1087–1090. https://doi.org/10.1055/s-0042-107248.
Varrecchia, T., Serrao, M., Rinaldi, M., Ranavolo, A., Conforto, S., De Marchis, C., Simonetti, A., Poni, I., Castellano, S., Silvetti, A., Tatarelli, A., Fiori, L., Conte, C., Draicchio, F., 2019. Common and specific gait patterns in people with varying anatomical levels of lower limb amputation and different prosthetic components. Hum Mov Sci 66, 9–21. https://doi.org/10.1016/J.HUMOV.2019.03.008.
Wang, H., Frame, J., Ozimek, E., Leib, D., Dugan, E.L., 2012. Influence of fatigue and load carriage on mechanical loading during walking. Mil Med 177, 152.
Winter, D.A., Sienko, S.E., 1988. Biomechanics of below-knee amputee gait. J Biomech 21, 361–367.
Woltring, H., 1986. A Fortran package for generalized, cross-validatory spline smoothing and differentiation. Advanced Engineering Software 8, 104–107.
Yang, F., Ban, R., Yang, F., 2022. Anterior load carriage increases the risk of falls in young adults following a slip in gait. Saf Sci 145. https://doi.org/10.1016/j.ssci.2021.105489.